

Excitation of the lowest lying 3B_1 , 1B_1 , 3A_2 , 1A_2 , 3A_1 and 1A_1 electronic states in water by 15 eV electrons

Michael J. Brunger^{a,*}, Penny A. Thorn^a, Laurence Campbell^a, Nicole Diakomichalis^a,
Hidetoshi Kato^b, Hirotomo Kawahara^b, Masamitsu Hoshino^b,
Hiroshi Tanaka^b, Yong-Ki Kim¹

^a ARC Centre for Antimatter-Matter Studies, SoCPES, Flinders University, GPO Box 2100, Adelaide, SA 5001, Australia

^b Physics Department, Sophia University, Chiyoda-ku, Tokyo 102-8554, Japan

Received 9 July 2007; received in revised form 12 September 2007; accepted 13 September 2007

Available online 19 September 2007

Abstract

We report absolute differential and integral cross-sections for excitation of the six lowest lying electronic states in water. The incident electron energy for this study was 15 eV and the scattered electron angular range, for the differential cross-section measurements, was $10 - 90^\circ$. Where possible comparison of the present cross-sections with the corresponding results from theory is made, the level of agreement between them being found to be somewhat marginal.

© 2007 Elsevier B.V. All rights reserved.

PACS: 34.80.Gs

Keywords: Cross-sections; Electronic states; Water

1. Introduction

In our companion papers to the present study, which looked at differential (DCS) and integral (ICS) cross-sections in the 20–200 eV electron energy range for excitation of the dissociative \tilde{a}^3B_1 , \tilde{A}^1B_1 , \tilde{b}^3A_1 and \tilde{B}^1A_1 electronic states [1,2], an extensive rationale for why electron impact studies on water are important was made. As a consequence we do not repeat that detail here except to note that electron collisions are fundamental processes in many phenomena involving water molecules [3].

A very nice summary of the available cross-sections for electron scattering from water (H₂O) was provided in the review of Itikawa and Mason [3], who noted that ‘to date no electron beam measurements have reported absolute values of the (electronic state) excitation cross-sections of H₂O’. The earlier work of Thorn et al. [1,2] and the present investigation have thus

sought, to some extent, to address this issue. From a theoretical perspective, however, there are significantly more results in the literature. These include the complex Kohn results from Gil et al. [4], a Schwinger multichannel [5] result for the \tilde{b}^3A_1 state, distorted wave computations again for the \tilde{b}^3A_1 electronic state [6,7] and some R-matrix results [8,9]. It is important to note that where there is overlap between the various theory DCS and ICS, they generally do not agree well with one another. This point provided further motivation for our current work.

Contrary to our description above for electron scattering from H₂O, there have been significant theoretical and experimental studies looking at the spectroscopy of the electronic states in water [1,2]. As we have noted and discussed these studies previously in Thorn et al. [1,2] we do not do so again here, except to highlight the pioneering energy-loss work from Trajmar et al. [10] and Chutjian et al. [11]. All these spectroscopic studies were vital in enabling us to deconvolve the respective electronic-state contributions to our measured energy-loss spectra, with a summary of these earlier spectroscopy investigations being found in Table 10 of Itikawa and Mason [3].

In this paper we extend our DCS and ICS measurements for the 3B_1 , 1B_1 , 3A_1 and 1A_1 electronic states down to an electron

* Corresponding author. Tel.: +61 8 8 8201 2958; fax: +61 8 8 8201 2905.
E-mail address: michael.brunger@flinders.edu.au (M.J. Brunger).

¹ Formerly of National Institute of Standards and Technology, Gaithersburg, MD 20899-8422, USA.

energy of 15 eV. In addition, we report the first cross-sections for excitation of the 3A_2 and 1A_2 electronic states. In the next section a very brief description of our measurement techniques and analysis procedures is given. Thereafter our results and a discussion of these results, including comparison to theory [4–9], is made. Finally some conclusions from our study are given in Section 4.

2. Experimental details

As most of the measurements reported here were made at Flinders University, and as the Flinders apparatus and procedures have been described many times before, only the most salient details of the Flinders-based spectrometer are provided. Please see reference [1] for a description of the Sophia University apparatus and methodology.

An electron monochromator [12] was utilised to perform our energy-loss measurements. Here a beam of H_2O , effusing from a molybdenum tube of 0.6 mm internal diameter, is crossed with a 15 eV beam of electrons. Elastically and inelastically scattered electrons at a given scattering angle (θ) are energy analysed and detected. The typical energy resolution of the monochromator was ~ 50 meV (FWHM), with incident beam currents into the interaction region being ~ 2 nA. The true zero scattering angle was determined as that about which the elastic scattering intensity was symmetric, with the estimated error in this procedure being $\pm 1^\circ$. The electron energy scale was calibrated against the 2^2S resonance in helium at 19.367 eV, and is thought to be accurate to better than 50 meV.

For our 15 eV incident electrons, energy-loss spectra were recorded at each θ over the range $\Delta E \sim -0.5$ to 10.5 eV. A typical spectrum, with the elastic peak suppressed for clarity, is plotted in Fig. 1. These spectra were collected by ramping the analyser in an energy-loss mode in conjunction with a multi-channel scaler, which stored the scattered signal as a function of energy loss. These data are now transferred to a Dec Alpha workstation for analysis. Each spectrum is then deconvolved by a computer least-squares fitting technique whose function is similar in detail to that of Nickel et al. [13], although adapted to accommodate the particular spectroscopy of H_2O [1,2](see

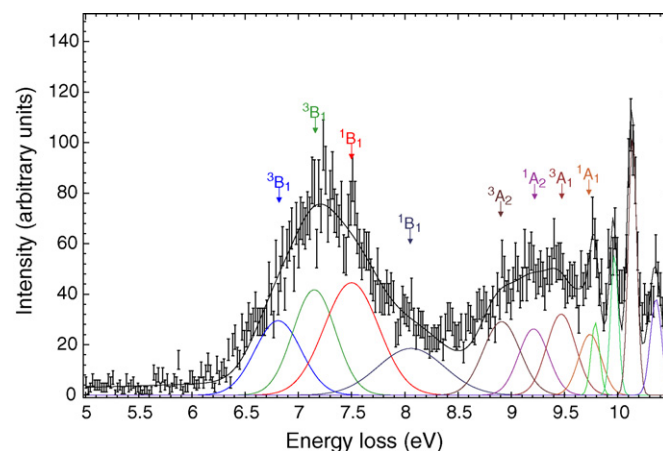


Fig. 1. Typical energy-loss spectrum for electron impact excitation of the electronic states of water. $E_0 = 15$ eV and $\theta = 50^\circ$. Note that the elastic peak has been suppressed for the sake of clarity. Also shown in this figure is our spectral deconvolution of this energy-loss spectrum.

also P.A. Thorn, Ph.D. Thesis, Flinders University, 2008, unpublished.). It should hence be apparent that an understanding of the spectroscopy of the electronic states of H_2O is absolutely crucial in this deconvolution process, for example to assign the peaks in the energy-loss spectra and to determine their respective profile shapes and widths. A comprehensive survey (see references [12–30] in reference [2]) on the spectroscopy of H_2O was therefore undertaken by Thorn (P.A. Thorn, Ph.D. Thesis, Flinders University, 2008, unpublished.), and this knowledge was used to fix as many of the deconvolution variables as was possible. An example of our spectral deconvolution is also given in Fig. 1. Note that as the respective line profiles of the \tilde{a}^3B_1 and \tilde{A}^1B_1 states are asymmetric [2,14], two symmetric Gaussian functions were required in the fit to correctly represent their form (see Fig. 1). In practice the fitting procedure yielded the ratio of the DCS for the inelastic feature of interest ($n' = ^3B_1, ^1B_1, ^3A_2, ^1A_2, ^3A_1, ^1A_1$), $\sigma_{n'}(15 \text{ eV}, \theta)$, to the elastic DCS $\sigma_0(15 \text{ eV}, \theta)$. That is:

$$R_{n'}(15 \text{ eV}, \theta) = \frac{\sigma_{n'}(15 \text{ eV}, \theta)}{\sigma_0(15 \text{ eV}, \theta)}. \quad (1)$$

Table 1

Present 15 eV differential ($\times 10^{-20} \text{ cm}^2/\text{sr}$) and integral ($\times 10^{-20} \text{ cm}^2$) cross-sections for electron impact excitation of the \tilde{a}^3B_1 , \tilde{A}^1B_1 , 3A_2 , 1A_2 , \tilde{b}^3A_1 and \tilde{B}^1A_1 electronic states in water

θ ($^\circ$)	DCS ($\times 10^{-20} \text{ cm}^2/\text{sr}$)					
	\tilde{a}^3B_1	\tilde{A}^1B_1	3A_2	1A_2	\tilde{b}^3A_1	\tilde{B}^1A_1
10	217.02 (49.40)	307.26 (65.88)	51.61 (11.08)	21.41 (5.63)	42.04 (8.86)	37.24 (8.69)
20	79.65 (14.91)	123.47 (23.43)	11.89 (2.72)	12.38 (3.14)	16.70 (3.23)	15.49 (2.91)
30	48.20 (11.39)	79.20 (23.52)	7.12 (4.41)	9.63 (4.49)	10.93 (4.76)	6.04 (4.70)
40	23.16 (4.33)	34.06 (6.11)	6.81 (1.96)	6.77 (1.41)	8.15 (1.59)	5.20 (1.32)
50	19.56 (3.55)	22.63 (4.20)	7.43 (1.50)	4.70 (0.97)	5.78 (1.04)	3.29 (0.90)
60	15.87 (3.38)	16.22 (3.50)	6.67 (1.44)	4.30 (1.23)	4.20 (0.85)	2.96 (0.58)
70	15.41 (2.91)	13.53 (2.52)	6.25 (1.29)	4.19 (0.78)	3.90 (0.89)	3.05 (0.55)
80	12.80 (2.43)	10.73 (1.87)	5.37 (0.95)	3.08 (0.54)	3.36 (0.59)	2.23 (0.49)
90	8.06 (1.43)	6.71 (1.34)	3.11 (0.71)	1.57 (0.28)	2.00 (0.41)	1.29 (0.43)
ICS	208.93 (44.27)	259.03 (61.19)	55.79 (21.08)	61.67 (30.75)	48.71 (12.75)	37.35 (13.64)

The absolute errors on the data are given in the parentheses.

It follows from Eq. (1) that the product $R_{n'}(15\text{ eV}, \theta) \times \sigma_0(15\text{ eV}, \theta)$ gives the required electronic-state DCS provided $\sigma_0(15\text{ eV}, \theta)$ is known. As was the case with our initial water studies [1,2], our preferred elastic H_2O differential cross-sections are those from Cho et al. [15]. Eq. (1) is only valid if the transmission response of the analyser remains constant, or is well characterised, over the energy loss and angular range studied. In this work we characterised the analyser response following the approach of Allan [16].

Care was also paid to the identification and quantification of all possible sources of error with our work, more details being found in Thorn et al. [1]. In this study the overall errors in our DCS typically ranged from ~ 20 to 50% , depending on the electronic state and scattering angle of interest. The errors on our ICS were typically in the range $\sim 21 - 50\%$.

3. Results and discussion

The present 15 eV differential and integral cross-sections for excitation of the $^3\text{B}_1$, $^1\text{B}_1$, $^3\text{A}_2$, $^1\text{A}_2$, $^3\text{A}_1$ and $^1\text{A}_1$ electronic states of water are listed in Table 1. A selection of these data, and any relevant corresponding theory, are also plotted in Figs. 2–6.

Considering Fig. 2(a) in more detail, we see that the independently measured present Flinders and Sophia $^1\text{B}_1$ DCS are in good agreement to within their respective uncertainties. Also plotted in this figure is the $^1\text{B}_1$ complex-Kohn theory DCS from Gil et al. [4]. It is clear from Fig. 2(a) that the theory overestimates the magnitude of the DCSs across all common θ . However, when the theory is scaled by a factor of 0.2 good shape agreement is found between the measurements and this scaled calculation. In Fig. 2(b) we plot the earlier 20 eV result from Thorn et al. [1]. In this case the theory scaling factor, to achieve good agreement between the measurements and calculation, is now 0.5. As the target description for the $^1\text{B}_1$ electronic state is the same at both 15 and 20 eV, we surmise that the complex-Kohn scattering mechanism description is more physical at 20 eV compared to 15 eV.

In Fig. 3(a) we now plot the present 15 eV $^1\text{A}_1$ electronic-state DCSs, while in Fig. 3(b) the corresponding 20 eV results from Thorn et al. [2] are shown. In both cases the relevant theory from Gil et al. [4] is also shown. A similar story as to that just described above for the $^1\text{B}_1$ state is also applicable for the $^1\text{A}_1$ state. Note, however, that the scaling factors required to give qualitative agreement between our $^1\text{A}_1$ DCS measurements and the theory of Gil et al. [4] are now much more significant (0.015 at 15 eV and 0.03 at 20 eV [2]). If we now concentrate on the 15 eV data alone, then it is apparent from Figs. 2(a) and 3(a) that the $^1\text{B}_1$ scaling factor is only 0.2 while the $^1\text{A}_1$ scaling factor is 0.015. As the reaction description, at least to first-order, is equivalent for both states at the common energy, we believe this significant difference in the scaling factors reflects that the $^1\text{B}_1$ target description of Gil et al. is superior to their $^1\text{A}_1$ target description. Rescigno (T.N. Rescigno, personal communication, 2006) had previously noted that many of the electronic states in water had both Rydberg and valence character. As a consequence he believed they would be difficult to characterise properly with

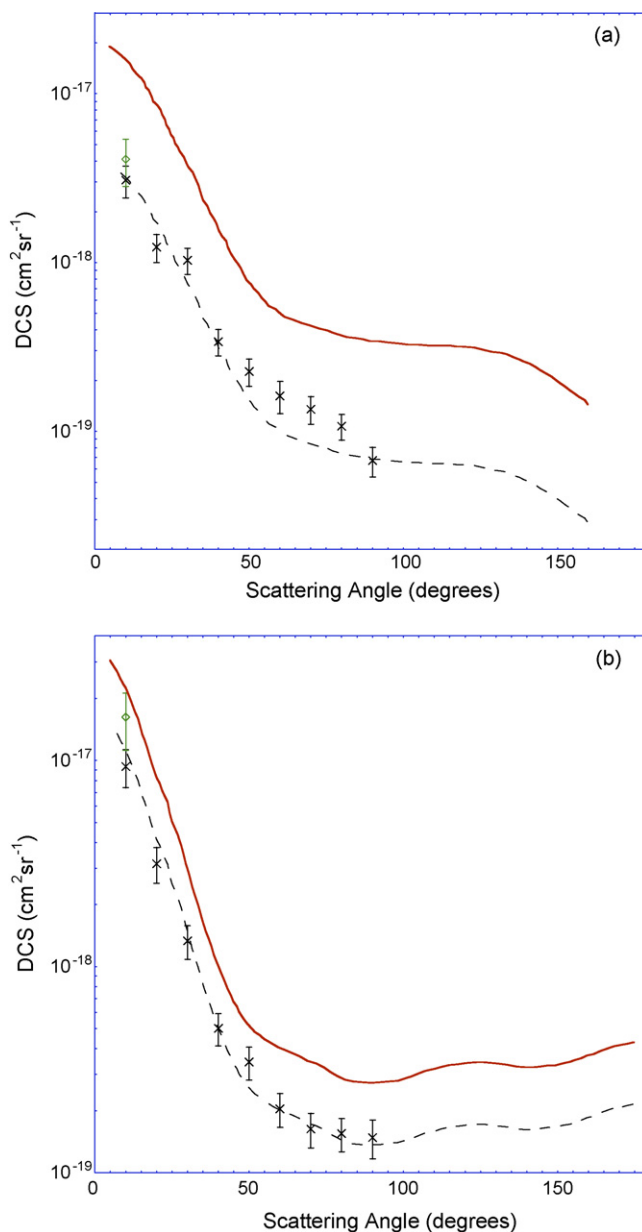


Fig. 2. Differential cross-sections for electron impact excitation of the $\bar{\text{A}}^1\text{B}_1$ electronic state in H_2O . (a) $E_0 = 15\text{ eV}$ with (x) present Flinders data, (\diamond) present Sophia data, (—) calculation by Gil et al. [4] and (---) calculation of Gil et al. [4] scaled by 0.2. (b) $E_0 = 20\text{ eV}$ with (x) Thorn et al. [1] data from Flinders, (\diamond) Thorn et al. [1] data from Sophia, (—) calculation by Gil et al. [4] and (---) calculation of Gil et al. [4] scaled by 0.5.

the relatively simple description of the target used in Gil et al. [4]. He also noted that some states in Gil et al. would be better described than others, with the results in Figs. 2 and 3 clearly supporting that notion.

We believe Fig. 4 represents the first time that any differential cross-sections have been reported, for electron impact excitation of the $^1\text{A}_2$ and $^3\text{A}_2$ electronic states. The angular distribution for the $^1\text{A}_2$ state (Fig. 4(b)) is in general strongly forward peaked, while (excluding the point at 10°) that for the $^3\text{A}_2$ state (Fig. 4(a)) is less so. The point at 10° in the $^3\text{A}_2$ DCS is interesting, as we would not have intuitively expected a triplet state to be forward

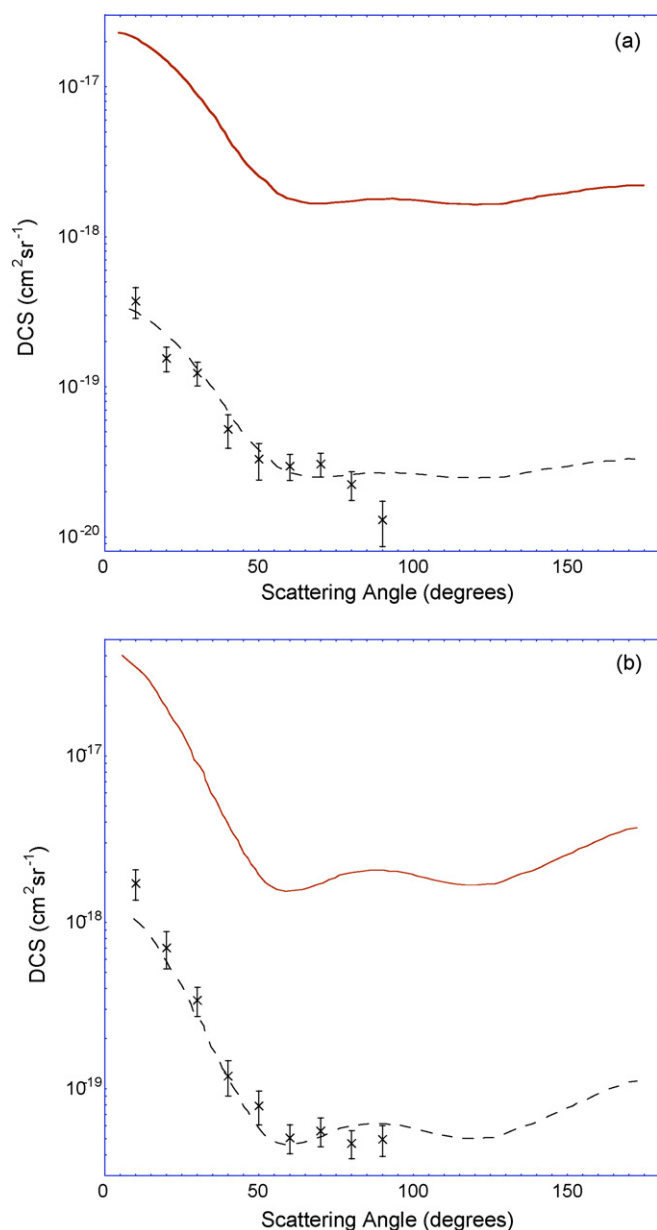


Fig. 3. Differential cross-sections for electron impact excitation of the \bar{B}^1A_1 electronic state in H_2O . (a) $E_0 = 15$ eV with (x) present Flinders data, (—) calculation by Gil et al. [4] and (---) calculation of Gil et al. [4] scaled by 0.015. (b) $E_0 = 20$ eV with (x) Thorn et al. [2] data, (—) calculation by Gil et al. [4] and (---) calculation of Gil et al. [4] scaled by 0.03.

peaked after excitation from a singlet ground-state. Thus, despite our best endeavours, the 3A_2 DCS at 10° may in fact be suffering from some 1A_2 contamination. Certainly some theory would be particularly welcome here to further establish the shape of the 3A_2 angular distribution.

In Figs. 5 and 6 we respectively plot the present ICS for the 3B_1 and 3A_1 electronic states. Also shown are the previous data from Thorn et al. [2] and the results of the theoretical calculations of Gil et al. [4], Pritchard et al. [5], Lee et al. [6,7], Morgan [8] and Gorfinkiel et al. [9]. In both cases all the relevant theories clearly overestimate the magnitude of the experimental ICS, at all common energies. This result is consistent with what would

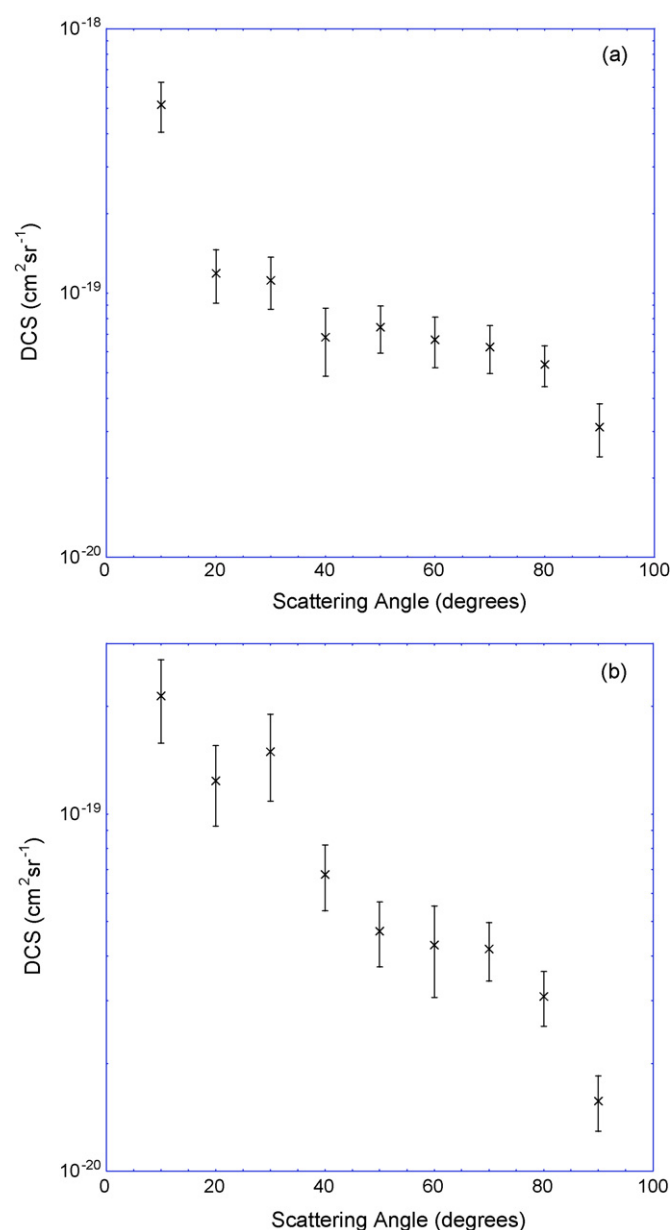


Fig. 4. Differential cross-sections for 15 eV electron impact excitation of the (a) 3A_2 and (b) 1A_2 electronic states in H_2O . The (x) present data from Flinders are shown.

be anticipated on the basis of the corresponding DCS data. While both these ICS are largely featureless, we thought it important to extend the measured ICS data base to closer to the respective electronic-state thresholds. The rationale for this follows from our foreshadowed atmospheric modelling and electron transport (swarm) phenomena studies [17], where near-threshold effects may be important.

The present 15 eV integral cross-sections, as listed in Table 1, were determined from the corresponding DCS data using the molecular phase shift analysis (MPSA) procedure of Campbell et al. [18]. This process extrapolated the measured DCS to 0° and 180° , before the usual integration was performed. Full details of this procedure, including safeguards to ensure unphysical results

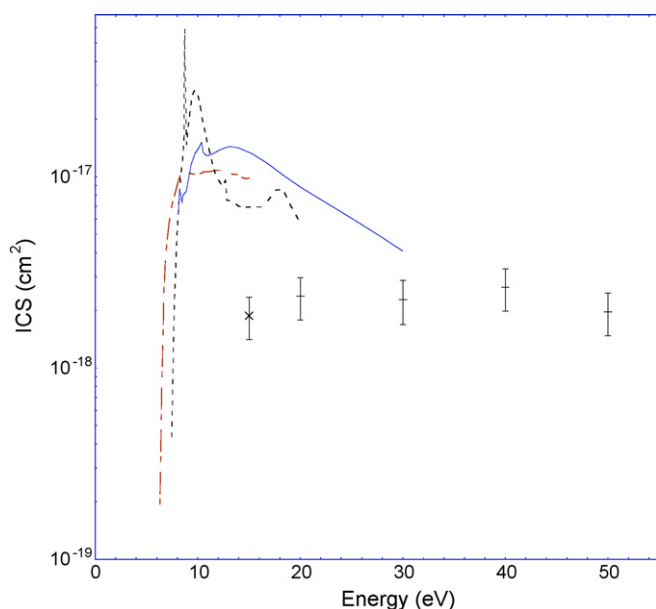


Fig. 5. Integral cross-sections (cm^2) for electron impact excitation of the \tilde{a}^3B_1 electronic state in H_2O . (x) Present data, (+) data of Thorn et al. [2], (—) calculation of Gil et al. [4], (---) calculation of Gorfinkiel et al. [9] and (-.-) calculation of Morgan [8].

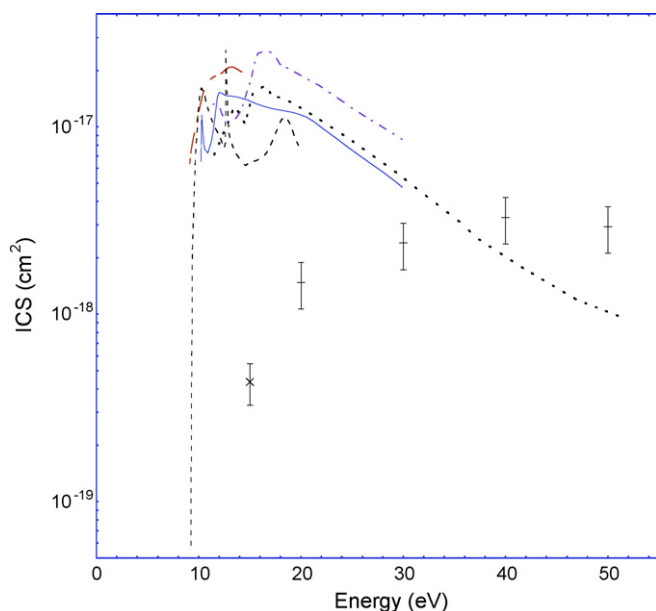


Fig. 6. Integral cross-sections (cm^2) for electron impact excitation of the \tilde{b}^3A_1 electronic state in H_2O . (x) Present data, (+) data of Thorn et al. [2], (—) calculation of Gil et al. [4], (---) calculation of Gorfinkiel et al. [9], (-.-) calculation of Morgan [8], (···) calculation of Lee et al. [6,7] and (---) calculation of Pritchard et al. [5].

are avoided, can be found in Campbell et al. [18] and so are not repeated here. Note, however, that Tennyson (J. Tennyson, personal communication, 2007.) recently found, for the case of elastic scattering in water, that the MPSA sometimes underestimated the ICS by as much as 30%, due to the very strong forward angle peaking in the elastic DCS. This is an important

point which needs to be borne in mind when considering the ICS data of Table 1.

4. Conclusions

We have reported absolute 15 eV differential and integral cross-sections for electron impact excitation of the 3B_1 , 1B_1 , 3A_2 , 1A_2 , 3A_1 and 1A_1 electronic states in water. Where comparison with theory at the DCS-level was possible, good qualitative (shape) agreement was found. However, the magnitude of the complex-Kohn calculations [4] was consistently larger than our DCS measurements. A similar picture also holds at the ICS-level where, over the common energy regime, all the theories [4–9] overestimate the magnitude of the relevant cross-sections. The present study, when combined with the results of Thorn et al. [1,2], suggest that current theoretical target descriptions need to be improved. Note, however, we fully concede that such improvements are likely to be non-trivial. Nonetheless, a renewed theoretical effort into the electronic-state excitation of water by electrons would be welcome.

Acknowledgements

This work was supported in part by the Australian Research Council. One of us (P.A.T.) thanks the Ferry Trust for her scholarship. We all thank Dr Tom Rescigno for his helpful comments regarding the interpretation of some aspects of our data. This work is dedicated to the memory of Dr Yong-Ki Kim who was tragically killed in a motor vehicle accident in late 2006.

References

- [1] P.A. Thorn, M.J. Brunger, P.J.O. Teubner, N. Diakomichalis, T. Maddern, M.A. Boloriazdeh, W.R. Newell, H. Kato, M. Hoshino, H. Tanaka, H. Cho, Y.-K. Kim, *J. Chem. Phys.* 126 (2007) 064306.
- [2] P.A. Thorn, M.J. Brunger, H. Kato, M. Hoshino, H. Tanaka, *J. Phys. B* 40 (2007) 697.
- [3] Y. Itikawa, N.J. Mason, *J. Phys. Chem. Ref. Data* 34 (2005) 1.
- [4] T.J. Gil, T.N. Rescigno, C.W. McCurdy, B.H. Lengsfeld III, *Phys. Rev. A* 49 (1994) 2642.
- [5] H.P. Pritchard, V. McKoy, M.A.P. Lima, *Phys. Rev. A* 41 (1990) 546.
- [6] M.T. Lee, S.E. Michelin, L.E. Machado, L.M. Brescansin, *J. Phys. B* 26 (1993) 203.
- [7] M.T. Lee, S.E. Michelin, T. Kroin, L.E. Machado, L.M. Brescansin, *J. Phys. B* 28 (1995) 1859.
- [8] L.A. Morgan, *J. Phys. B* 31 (1998) 5003.
- [9] J.D. Gorfinkiel, L.A. Morgan, J. Tennyson, *J. Phys. B* 35 (2002) 543.
- [10] S. Trajmar, W. Williams, A. Kuppermann, *J. Chem. Phys.* 58 (1973) 2521.
- [11] A. Chutjian, R.I. Hall, S. Trajmar, *J. Chem. Phys.* 63 (1975) 892.
- [12] M.J. Brunger, P.J.O. Teubner, *Phys. Rev. A* 41 (1990) 1413.
- [13] J.C. Nickel, P.W. Zetner, G. Shen, S. Trajmar, *J. Phys. E* 22 (1989) 730.
- [14] R. Mota, R. Parafita, A. Giuliani, M.-J. Hubin-Franskin, J.M.C. Loureço, G. Garcia, S.V. Hoffmann, N.J. Mason, P.A. Ribeiro, M. Raposo, P. Limão-Vieira, *Chem. Phys. Lett.* 416 (2005) 152.
- [15] H. Cho, Y.S. Park, H. Tanaka, S.J. Buckman, *J. Phys. B* 37 (2004) 625.
- [16] M. Allan, *J. Phys. B* 38 (2005) 3655.
- [17] M.J. Brunger, W.L. Morgan, P.A. Thorn, *Bull. Am. Phys. Soc.* 52 (2007) 42.
- [18] L. Campbell, M.J. Brunger, A.M. Nolan, L.J. Kelly, A.B. Wedding, J. Harrison, P.J.O. Teubner, D.C. Cartwright, B. McLaughlan, *J. Phys. B* 34 (2001) 1185.